Journal of Chromatography A, 1601 (2019) 375–384

Contents lists available at ScienceDirect

Journal of Chromatography A

journal homepage: www.elsevier.com/locate/chroma

Capillary zone electrophoresis-native mass spectrometry for the quality control of intact therapeutic monoclonal antibodies

Victor Le-Minh [a], N.Thuy Tran [a], Ali Makky [b], Veronique Rosilio [b], Myriam Taverna [a], Claire Smadja [a,*]

[a] Institut Galien Paris Sud, UMR CNRS 8612, Protein and Nanotechnology in Analytical Science, CNRS, Univ. Paris-Sud, Univ. Paris-Saclay, 5 rue Jean-Baptiste Clément, 92290 Châtenay-Malabry, France
[b] Institut Galien Paris Sud, UMR CNRS 8612, Surface Physical Chemistry, CNRS, Univ. Paris-Sud, Univ. Paris-Saclay, 5 rue Jean-Baptiste Clément, 92290 Châtenay-Malabry, France

ARTICLE INFO

Article history:
Received 14 February 2019
Received in revised form 18 May 2019
Accepted 26 May 2019
Available online 28 May 2019

Keywords:
Therapeutic mAbs
CZE-native MS
Folding
Unfolding
Dimers
Stability
AFM

ABSTRACT

Therapeutic monoclonal antibodies (mAbs) are complex glycoproteins and ensuring their safety, efficacy and quality is still challenging. Indeed, during their manufacturing process, they are exposed to several stresses that can lead to their denaturation, misfolding or dimerization. We report here a new method based on capillary electrophoresis coupled to native mass spectrometry (MS) with a sheath liquid interface to analyze an intact therapeutic mAb, Infliximab, under non-denaturing conditions that preserve its conformational heterogeneity as well as self-association without inducing further unfolding / denaturation. For capillary zone electrophoresis (CZE) separation, a triple layer coating using polybrene-dextran sulfate-polybrene was employed. A sheath liquid composed of isopropanol - water - acetic acid with a flow rate of 10 μL min^{-1} and mild MS conditions allowed optimal signal intensities. A specific mass spectrum was obtained for each Infliximab conformation in a "stressed" formulated preparation. This is the first time that within a single analysis different conformational states, i.e. native and unfolded monomers as well as dimers are simultaneously detected. The results and the lack of analytical bias arising from the CZE-MS conditions were confirmed by using atomic force microscopy (AFM) as an orthogonal technique. A middle-up approach combined to CZE-MS analysis of the stressed samples suggested that the dimer formation involved mostly Fab-Fab interactions.

© 2019 Elsevier B.V. All rights reserved.

1. Introduction

Therapeutic monoclonal antibodies (mAbs) are one of the key topics in pharmaceutical industry with an important growth rate, especially in cancer and chronic inflammatory therapies [1]. The success of these biopharmaceuticals is related to their capacity to specifically interact with their target with relatively low adverse effects [2]. However, mAbs are complex glycoproteins with a wide range of potential microheterogeneities leading to significant challenge to ensure their safety, efficacy and quality from their manufacturing, storage until finally patient administration. Indeed, during their manufacturing and storage, mAbs are exposed to several stresses such as extreme pHs, high temperatures, light exposure, mechanical agitation or contact with various surfaces and materials. Such exposures can alter mAbs conformation, leading to their misfolding, denaturation, dimerization and aggregation. These generated conformational variants can potentially induce immunogenicity and impact mAbs efficacy and safety [3,4]. This type of structural variants, which appear besides charge, glycosylated, truncated, glycated variants are also classified as product variants and can be considered as critical quality attributes that could influence mAbs toxicity, immunogenicity, efficacy and their mechanism of action.

An extensive literature has reported analytical approaches to assess charge and size variants of mAbs as part of their quality control and stability evaluation [5–7]. Many studies have been devoted to small oligomer detection (e.g dimers, trimers) in mAbs preparation using SEC [8]. However, the detection of denatured mAbs is still difficult. Indeed, unfolded or misfolded forms are prone to self-association with the possibility to form dimers and small size oligomers inducing *in vivo* immunogenicity. To detect these specific mAbs impurities (conformers and dimers), bottom-up and middle-up approaches are precluded. Only native and mild analytical conditions can preserve weak non-covalent assemblies. Native

* Corresponding author.
E-mail address: claire.smadja@u-psud.fr (C. Smadja).

https://doi.org/10.1016/j.chroma.2019.05.050
0021-9673/© 2019 Elsevier B.V. All rights reserved.

mass spectrometry (MS) was introduced for the first time in 2004 as one of the emerging approaches able to address this challenge [9]. The term "native MS" could refer nowadays to conditions that maintain mAbs in their original folded or unfolded state prior to MS analysis and also as much as possible during MS process [10]. Since only two years, a few liquid chromatography (LC) methods hyphenated to native MS and applied to IgG or therapeutic mAbs have been proposed [11]. Detecting non-covalent oligomers when using MS can indeed constitute a real challenge. Other approaches used Size Exclusion Chromatography (SEC) coupled to off-line native MS to allow both identification and quantification of size variants such as dimers, trimers and tetramers of a model bispecific antibody [12]. Ehkirch et al. developed recently an on-line coupling of SEC to native ion mobility spectrometry (IMS) IMS-MS to analyze pH-stressed trastuzumab which provided information on the monomeric mAbs and also on small oligomers [13]. SEC hyphenated to multi-angle scattering (MALS) is also a reliable method widely used to detect and separated small oligomers [14]. Although, LC—MS/MS and SEC-MALS can provide information about mAbs size variants (e.g. small oligomers), no conformational modifications such as denaturation or misfolding of mAbs have been detected yet by these approaches.

Besides these techniques, capillary zone electrophoresis (CZE) hyphenated to native-MS combining high separation efficiency and mass selective detection has recently attracted attention. Indeed, a recent interlaboratory study, composed by 13 independent laboratories (academic and private companies), evaluate the robustness of CE-MS for peptide mapping. The statistical evaluation, following ISO 85725-2 guidelines, showed that CE-MS method was robust, allowing thereby its transfer to multiple laboratories [15]. CE can be employed under mild conditions, without organic solvent, which is of particular interest to study conformers and small non-covalent oligomers. In addition, very few works on intact therapeutic mAbs analysis by CZE-MS have been reported until now [16–20]. Han et al. developed a CZE-MS with a sheath liquid (SL) interface method to analyze a non-therapeutic mAb, IgG1 but this protein was modified before analysis by reduction and deglycosylation [17]. Moreover, the denaturing conditions employed for mAbs (by using an acidic buffer) were not compatible with the preservation of the initial states of mAbs. More recently, two sheathless CZE-ESI-MS methods were developed to analyze intact commercial mAbs. These studies allowing an efficient characterization of mAbs glycoforms were performed under denaturing conditions [20,21]. A pioneering approach relying on sheathless CZE- native MS has been recently proposed to analyze one therapeutic mAb (trastuzumab) under native conditions [22,23]. This method revealed the presence of monomers and traces of dimeric species. The origin of the dimer species was not explored, and no evidence was provided to demonstrate that the dimerization process did not occur during the MS experiments. To our best knowledge, no CZE-native MS method allowing the simultaneous detection of different intact mAbs states (folded, unfolded and dimers) in a formulated therapeutic mAbs has been proposed until now.

In this study, we investigated on-line CZE-native MS with, this time, a SL interface to analyze and detect simultaneously in one commercial stressed mAb (infliximab) the native forms as well as all the monomeric conformers that could be considered as product impurities (unfolded, misfolded, partially folded) together with small oligomers. For this purpose, we investigated non-denaturing conditions which (i) favor electrospray ionization efficiency, (ii) increase mAbs protonation, (iii) minimize mAbs adsorption on the capillary while preserving the original state of the mAbs. A triple layer coating proposed by Haselberg et al. for CZE-MS of basics proteins was exploited, for the first time for mAbs [24]. The nature of the dimer association was also investigated by CZE-MS employing a middle-up approach. An orthogonal method, atomic force microcopy (AFM) was employed to verify that the oligomers observed in CZE-MS were not generated in the MS source.

2. Materials and methods

2.1. Materials

Polybrene 94% (Hexadimethrine bromide) (PB), dextran sulfate sodium salt (M.W. ~200 000) (DS), sodium chloride and sodium di-hydrogenphosphate, hydrochloric acid, sodium hydroxide (all reagent grade) were purchased from Sigma-Aldrich (St. Louis, MO, USA). Ultrapure water, methanol, iso-propanol, acetonitrile, 100% acetic acid and 25% ammonium hydroxide (v/v) (all MS grade) were obtained from Merck (Darmstadt, Germany). USP grade solutions as sterile water for injection and 0.9% NaCl solution were provided by Laboratoire Aguetttant (Lyon, France) and Fresenius Kabi France (Sèvres, France), respectively. FabRICATOR (Ides) was purchased from Genovis AB (Lund, Sweden). The Remicade (Infliximab) was purchased from Janssen Biologics B.V. (Leiden, The Netherlands)

Coating solutions and rinsing solution for AFM experiments were prepared with milli-Q water using a Direct-Q3 UV purification system (Millipore, Milford, MA, USA). The 0.2 μm nylon filter was obtained from VWR (Radnor, PA, USA).

2.2. Apparatus

2.2.1. CZE-MS

CZE-MS experiments were performed using a 7100 Agilent capillary electrophoresis and ESI-QTOF 6540 mass spectrometer (Agilent Technologies, Santa Clara, CA, USA). A 60 cm silica capillary (i.d. 50 μm) was used. CZE-MS coupling was performed using a co-axial SL electrospray interface from Agilent Technologies. Mass Hunter B.07.00 software was employed to analyze the MS data.

2.2.2. AFM

AFM experiments were performed using a Nanowizard® Ultra-speed AFM (JPK instruments, Berlin, Gemany). The samples were deposited onto a muscovite mica grade V1 (Ted pella, Redding, CA, USA). Gold coated silicon cantilevers PPP-NCH-AuD (Nanosensors, Neuchâtel, Switzerland) with a spring constant of ~42 N m^{-1} and a tip curvature radius of ~10 nm were used. Data acquisition was carried out manually using JPK Data Processing software.

2.3. Methods

2.3.1. Preparation of native and stressed Infliximab

Reconstituted infliximab was prepared according to manufacturer guidelines of Remicade. Infliximab lyophilized powder was diluted in sterile water for injection to obtain a concentration of 10 mg mL^{-1}. The solution was then diluted in 0.9% NaCl solution (under aseptic conditions) to obtain a concentration of 1 mg mL^{-1} (6.7 μM) or 2 mg mL^{-1} (13.4 μM). The solution was finally dialyzed for 1 h using a 10 kDa molecular weight cut-off Slide-A-Lyzer cassette (Thermo Fischer Scientific, Rockford, USA) against 10 mM ammonium acetate buffer pH 6.5 at 4 °C. The dialyzed solution was immediately analyzed. Stressed mAbs were prepared by storing reconstituted infliximab (2 mg mL^{-1}) at 4 °C for 6 months (protected from light). This stress has been chosen to reproduce conditions encountered during a long-term storage in hospitals. We could have chosen harsher and faster stress, but as the physical degradation pathway depends strongly on the nature of the stress, this would have led to different conclusions.

2.3.2. Capillary coating procedure

The fused-silica capillary was preconditioned by flushing 10 min at 50 psi with successively 1 M HCl, 1 M NaOH, MeOH, 0.1 M NaOH

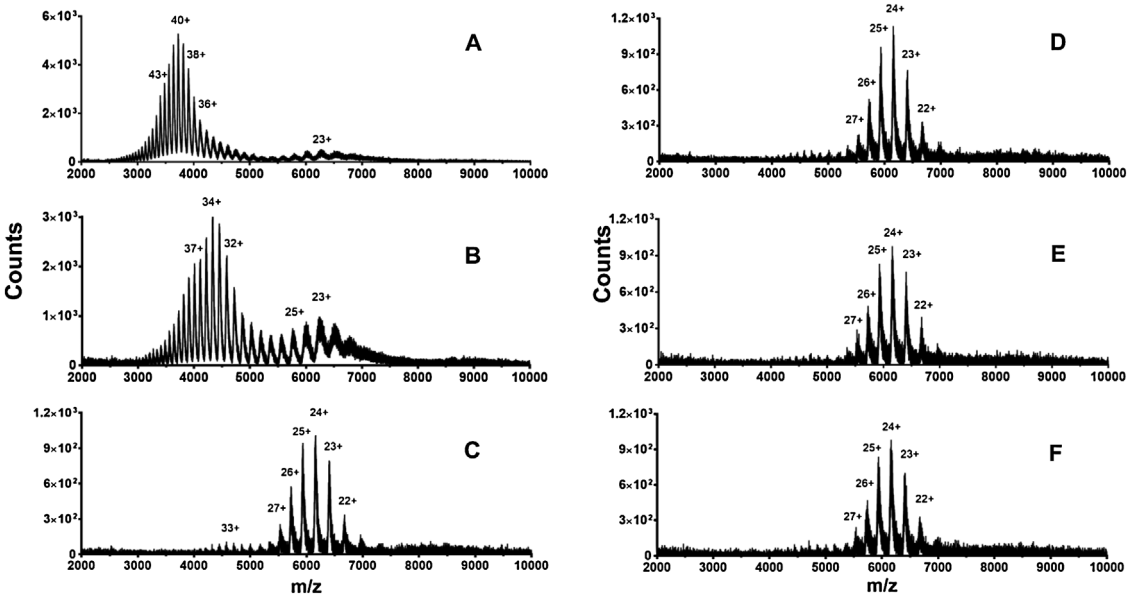


Fig. 1. MS spectra of dialyzed Infliximab (2 g L^{-1}) obtained by CZE-ESI-MS using different BGE pHs (A) 40 mM formic acid pH 1.8; (B) 40 mM acetic acid pH 3.0; and 40 mM ammonium acetate (C) pH 4.0, (D) pH 5.0, (E) pH 6.0, and (F) pH 7.0.
CE conditions: PB-DS-PB capillary (50 μm x60 cm), −12 kV, 20 °C
MS conditions: drying gas. 200 °C – 8 L min^{-1}, sheath gas 150 °C – 6 L min^{-1}, nebulizer pressure 10 psig, transferred capillary, nozzle, fragmentor and skimmer voltages were set at 3500 V, 2000 V, 300 V and 200 V, respectively; Sheath liquid: 10 μL min^{-1}, IPA/water/acetic acid 50:50:0.1 (v/v/v).

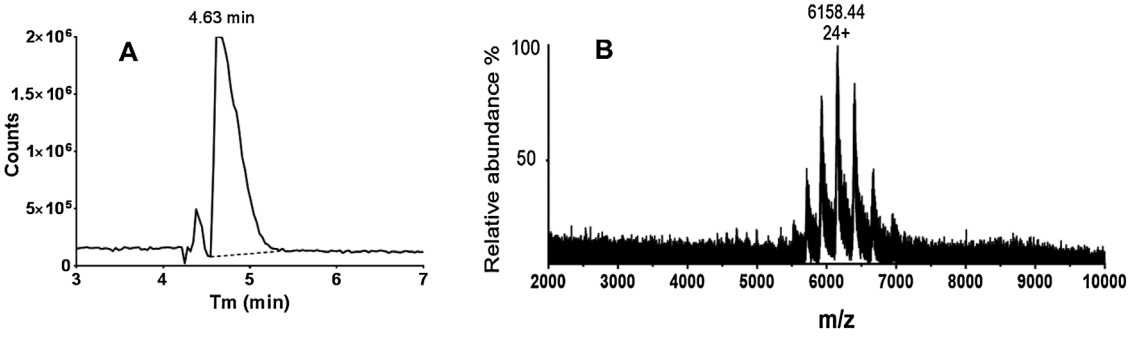


Fig. 2. CZE-MS analysis of fresh dialyzed Infliximab (2 mg mL^{-1}). (A) Total ion chromatogram (B) MS spectrum. Experimental conditions as mentioned in Fig. 1.

and deionized water. A triple layer cationic coating based on PB-DS-PB was adapted from the protocol described by Haselberg et al. [24]. Solutions of 10% w/v PB and 3% w/v DS in deionized water were freshly prepared and filtered through a 0.2 μm nylon membrane before the coating process. To ensure a good coating stability, the polymer solution rinse times were extended to 30 min at 10 psi, and 60 min incubation was performed after each polymeric solution flushing. The triple layer was prepared only once, and capillary wall was not re-coated before every single run as preconized by Haselberg et al. [24].

2.3.3. CZE-MS

Analysis of mAbs were performed on the triple coated capillary. Hydrodynamic injection was performed at 1.44 psi for 20 s (4.3% of capillary volume). The separation was performed using a 40 mM (ionic strength) ammonium acetate solution at pH 6.0 as BGE (buffer capacity 4.2 mmol.L^{-1}.pH). The separation voltage was −12 kV and the capillary temperature was set at 20 °C. Between runs the capillary was rinsed with the BGE at 13.7 psi for 5 min.

The SL was a mixture of water-isopropanol-acetic acid 50:50:0.1 (v/v/v), delivered at a flow-rate of 10 μL min^{-1}. The positive ionization mode was chosen using an ESI voltage of 3500 V. Nebulizer pressure was set at 10 psig. Flow and temperature of sheath gas (N_2) were set at 6 L min^{-1} and 150 °C, respectively. A drying gas temperature of 200 °C and flow (N_2) at 8 L min^{-1} were employed. The nozzle voltage was set at 2000 V. For the detector parameters, the micro-channel plate value was set at 900. Profile mass spectra were collected from 2000 to 10,000 *m/z* and a pusher rate of 2 GHz. The acquisition rate employed was 0.4 spectrum s^{-1}.

2.3.4. AFM measurements

Fresh and storage-stressed Infliximab samples were diluted in deionized water to obtain a concentration of 2 μg mL^{-1}. 100 μl of 2 μg mL^{-1} Infliximab were deposited onto freshly cleaved mica substrates and left to incubate for 1–2 min. Afterwards, the sub-

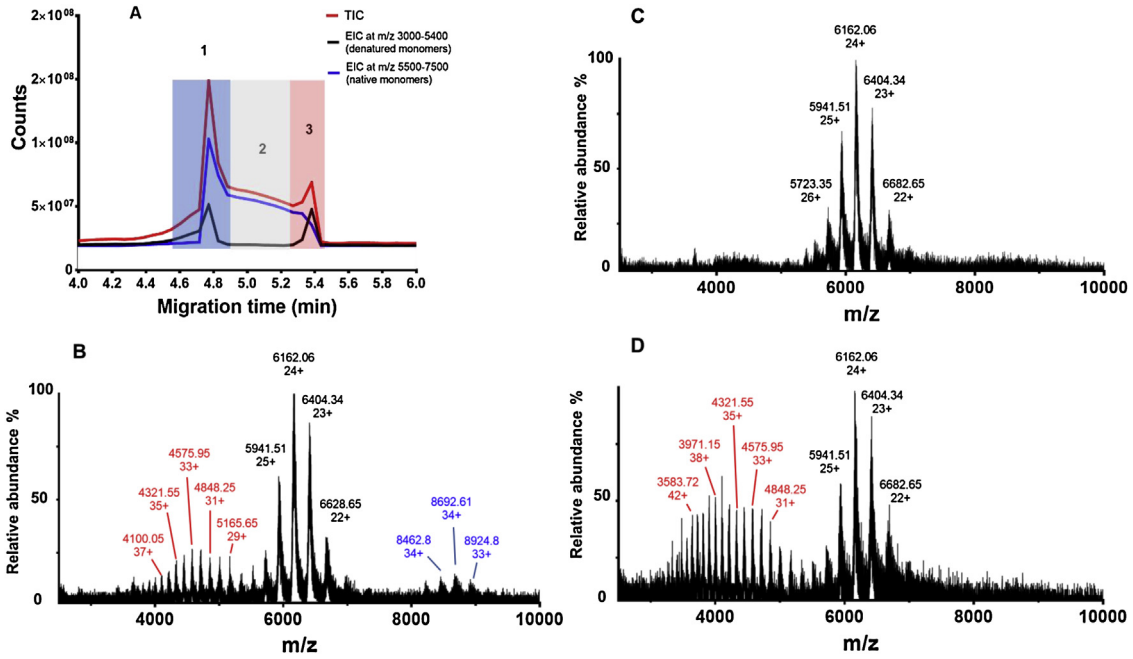


Fig. 3. Stressed Infliximab (2 mg mL^{-1}) analysis by CZE-MS. (A): Total ion chromatogram (red line), Extracted ion chromatogram (EIC) of folded Infliximab (5500–7000 *m/z*) (blue line), EIC of unfolded Infliximab (3000–5500 m/z) (black line). Mass spectra of (B) region 1 (4.5–4.9 min), (C) region 2 (4.9–5.3 min), (D) region 3 (5.3–5.5 min) from the TIC. Experimental conditions as mentioned in Fig. 1 (For interpretation of the references to colour in this figure legend, the reader is referred to the web version of this article).

strates were gently rinsed with 200 μl of ultrapure water and dried under nitrogen stream. The AFM imaging of antibody samples was performed at room temperature (20 ± 1 °C) and ambient humidity (RH ~35%) using an hydrophilic surface (mica) without any special control in amplitude modulation AFM (AM-AFM) in attractive regime [25,26] by applying low force settings [27] (90–95% of the free amplitude A ~20 nm). In AFM modulation, the tip-surface distance regulation was performed to maintain constant the amplitude to a precise set-point. Samples imaged in this way are not "dried" since they are coated with a thin water film, which can leave biomolecules in a hydrated state as demonstrated recently in our AFM study of amyloid fibrils [28]. We can reasonably assume that observation made on these wetted surfaces is close to what happens in solution.

For each sample, at least three different substrates at three different spots were systematically imaged at high resolution (2 μm × 2 μm, or 1 μm × 1 μm, 1024 × 1024 pixels) by AFM and their morphology (height and width) was analyzed manually with the JPK Data Processing software using the line profile measurement option. For determination of the lateral dimension of monomeric antibodies, the widths were measured manually at the full width at half maximum to reduce the tip convolution.

3. Results and discussion

3.1. Method development

The most important challenge to detect mAbs monomeric folded forms or dimers is to select: (i) non-denaturing separation and ESI conditions to maintain mAbs in their native or original state, (ii) sheath-liquid composition leading to the optimal detection sensitivity and mAbs ionization, (iii) mild MS parameters to prevent in-source dimers/oligomers dissociation, monomers association as well as unfolding or denaturation.

To reduce as much as possible the mAb adsorption onto the capillary wall, a triple layer coating (PB-DS-PB), adapted from Haselberg et al. has been employed for the CZE separation [24]. In addition, the high electroosmotic flow induced by this cationic coating allowed mAbs migration without any additional pressure which would be detrimental to the analysis performances. We first optimized the BGE to analyze dialyzed reconstituted Infliximab. Under acidic and neutral conditions, a broad peak was observed (Fig. S1 A–F). Deconvolution spectra showed a main molecular mass of 149,096 ± 109 Da, which is in agreement with the theoretical molecular mass of Infliximab. Fig. 1 compares the MS spectra of dialyzed Infliximab at various BGE pHs. Using acidic BGEs (40 mM formic acid pH 1.8; 40 mM acetic acid pH 3.0 and 40 mM ammonium acetate pH 4.0), Infliximab displayed a bimodal MS spectrum. At pH 1.8, the first envelope has a charge state distribution centered at 40+ and a wide mass range (2500–5500 m/z) whereas the second one exhibits a charge state distribution centered at 23+ and a narrower mass range (5500 to 7000 *m/z*) (Fig. 1A). These results are in agreement with previous studies showing by ESI-MS that the decrease of the pH to 2.6 in solution, generated for proteins like cytochrome C, a higher charge state distribution with a bimodal distribution corresponding to two co-existing forms; unfolded and folded [29]. Parallelly, these authors demonstrated by complementary techniques (fluorescence, circular dichroism and absorption spectroscopy) that acidic conditions (pH 2.6) induced denaturation of the cytochrome C through the breakdown of the secondary and tertiary structure. Acidic pHs are known to induce higher protonation of proteins. Protonation and unfolding are likely to be intricated. jhConsidering that for a given native protein with a molecular mass M, the theoretical maximum charge state (Z) can be evaluated as $Z = 0.079 \times M^{1/2}$ [30], we estimated that for the native mAbs this value was 30+. The charge state of the second signal could correspond to the folded native mAbs. Indeed, folded mAbs exhibit a small number of charges on its surface, and this is also

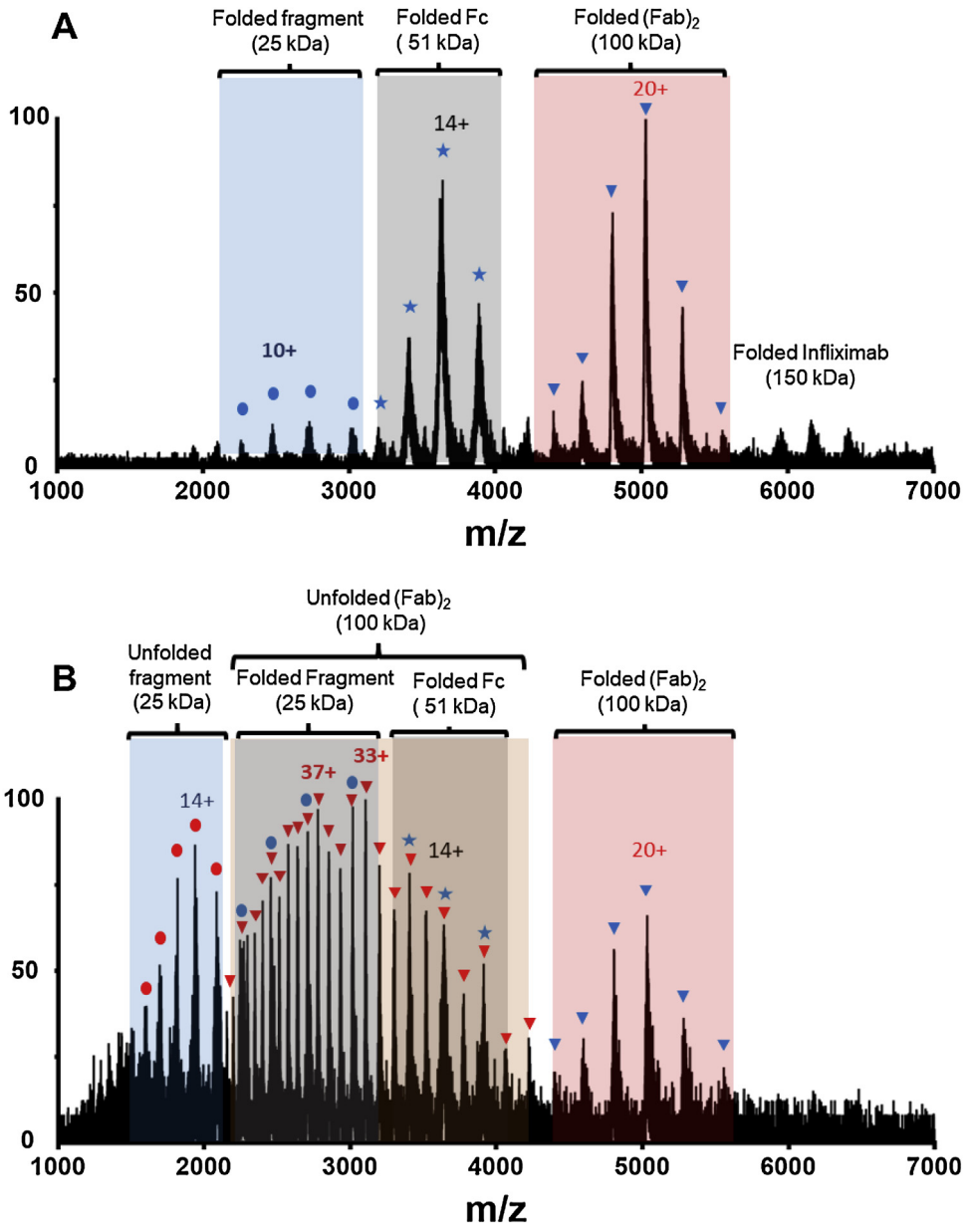


Fig. 4. Mass spectra of reduced and IdeS treated Infliximab analyzed by CZE-MS. (A) Fresh Infliximab, (B) storage stressed Infliximab. Peaks: (●) Folded Fc/2, (★) Folded Fc, (▼) Folded F(ab)$_2$, (▼) denatured F(ab)$_2$, (●) Denatured Fc/2. Experimental conditions as mentioned in Fig. 1.

accompanied by narrower distribution of charge states. The first signal corresponded rather to a fully unfolded mAbs. Indeed, when mAbs is fully unfolded, it exposes more sites to protonation leading to a high charge state distribution with a wide mass range in the mass spectrum. Higher protonation of a "folded" forms solely should probably not induce a so important charge state shift. In addition, the fact that two forms are co-existing on the MS spectrum argues for the presence of coexisting unfolded and folded forms. At pHs 3.0 and 4.0, the first signal exhibited a distribution shift to higher *m/z* values compared to pH 1.8 (from 40+ at pH 1.8 to 34+ at pH 3.0 and pH 4.0) (Fig. 1B–C) and also a decreased signal intensity, probably due to partial unfolding of the mAb. At pH 4.0 this partial unfolded form exhibited an extremely low signal. The second signal, corresponding to native monomer, was increased from pH 3.0 to pH 4.0. At pH ranging from 5.0 to 7.0 (BGE 40 mM ammonium acetate) (Fig. 1D–F), only one envelope related to the folded mAbs was observed. These results confirm that the high charge state distribution observed at acidic pHs corresponds to a partially unfolded or totally denatured mAbs as previously described by Sousa et al. [31].

We also observed that the signal intensity was slightly reduced, when BGE pHs raised from 5.0 to 7.0, close to Infliximab pI (7.6), probably due a small reduction of ionization efficiency and an increasing background noise. We compared two different types of BGE ammonium acetate and ammonium bicarbonate (40 mM ionic strength, pH 6.0). Results showed similar CE-native MS spectra for both buffers. However, it is important to note that ammonium bicarbonate potentially favor protein unfolding during ESI process [32]. Consequently, for all the following CZE-MS experiments, a BGE at pH 6.0 composed of 40 mM ammonium acetate was chosen as a compromise between the signal intensity and the preservation of native conditions. In this condition, the coating stability was

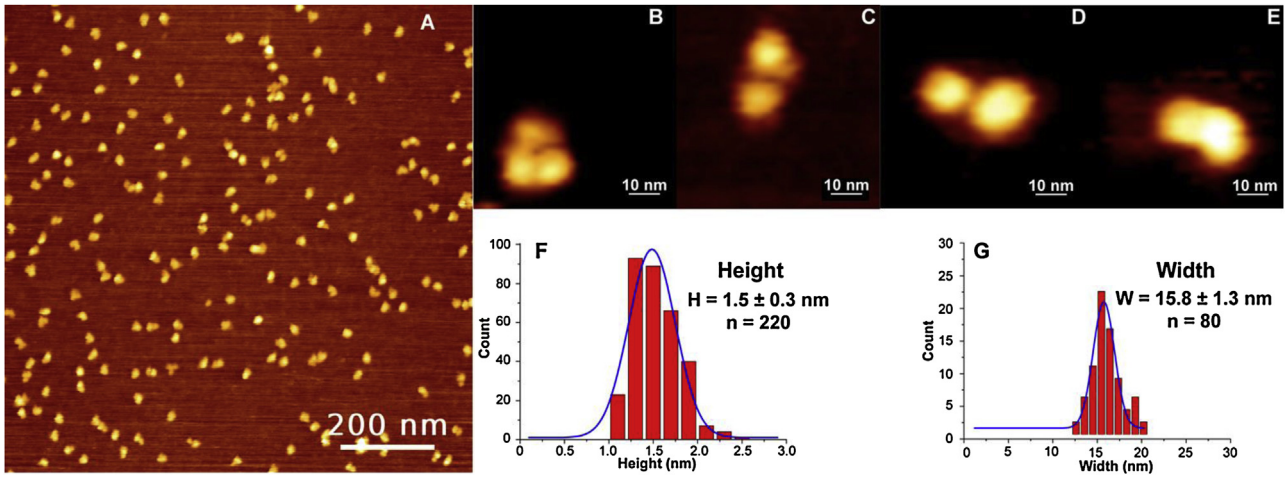


Fig. 5. (A) AM-AFM topography image of Infliximab monomeric forms adsorbed onto mica surface performed in ambient conditions. (B), (C), (D) and (E) images of individual antibodies with different orientation. Histograms of height (F) and (G) width of infliximab monomeric antibodies.

assessed. An excellent repeatability of Infliximab migration times was obtained with RSD below 0.64% (n = 8) for CZE-MS (Fig. S1G).

We then investigated the impact of the SL composition and flow rate on the ionization behavior of Infliximab using direct infusion in order to enhance the sensitivity of MS while preventing denaturation or self-association [33]. To favor sensitivity detection of mAbs, SL containing both acids and organic solvents are generally preferred as they allow maximum protonation of the amino acid ionizable groups. First, the influence of different solvents, acetonitrile, methanol and isopropanol (IPA) has been compared. For this purpose, we employed for SL a solvent/water ratio of 50:50 v/v. As expected, methanol and acetonitrile induced Infliximab denaturation, leading to the detection of the envelope corresponding to the unfolded mAbs (Fig. S2). In contrast, IPA did not induce any denaturation. Therefore, different ratios of IPA/water have been tested from 10:90 to 70:30 (v/v). The highest signal intensity for the native Infliximab was obtained for IPA/water ratios between 50:50 to 70:30 (v/v), and no unfolded form was observed in these conditions, despite the high content of IPA. Therefore, SL containing 50% of IPA has been employed in the following experiments. The influence of acidic additives (acetic and formic acids) in the SL was also tested at different proportions to further increase the signal intensity. Experiments showed that the detection sensitivity was improved and no mAbs unfolding was observed by using a SL containing 0.1% acetic acid in IPA/water 50:50 mixture. As the major drawback of SL is related to sample dilution effect, several flow-rates from 1 to 20 $\mu L\,min^{-1}$ have been tested. The signal intensities linearly increased with flow rates ranging from 1 to 10 $\mu L\,min^{-1}$ and then attained a plateau. However, Infliximab denaturation was observed at flow rates over 15 $\mu L\,min^{-1}$ (Fig. S2). To explain this phenomenon, two hypotheses could be proposed. First, a higher SL flow rate induces a higher proportion of acetic acid and IPA leading thereby to mAbs denaturation. Secondly, with a coaxial sheath liquid interface, an ionic boundary at the capillary outlet is formed due to the migration of sheath liquid counterions in the capillary [34]. At higher flow rate this ionic boundary zone might increase, favoring further mAbs denaturation. Therefore, a flow rate of 10 $\mu L\,min^{-1}$ was selected as a compromise between signal intensity and folded mAbs preservation.

Taking into account that MS parameters should be finely tuned to prevent dissociation of non-covalent complexes or denaturation of monomeric mAbs from solution into gas phase, both drying gas and sheath gas were lowered from 250 °C (8 L min^{-1}) to 200 °C (8 L min^{-1}) and from 295 °C (8 L min^{-1}) to 150 °C (6 L min^{-1}), respectively. The signal intensity increased with the nebulizer pressure ranging from 1 to 10 psig and remained constant for 10–20 psig. As the nebulizer gas pressure could cause possible siphoning effects during CZE-MS analysis, inducing unstable electrospray, the value of 10 psig was selected. A good ion transmission efficiency was achieved when the transfer capillary and the skimmer voltages were set at 3500 V and 200 V, respectively. An appropriate fragmentor voltage was selected at 300 V to minimize in-source induced collision dissociation while enhancing the signal intensity of Infliximab.

Therefore, the developed CZE-MS method using a BGE at near physiological conditions (40 mM ammonium acetate pH 6.0) and a SL composed of IPA/water/acetic acid, 50:50:0.1 v/v/v delivered at the flow rate 10 $\mu L\,min^{-1}$ and optimized and mild MS conditions described above was applied to the analysis of a fresh reconstituted Infliximab. No envelope corresponding to unfolded monomer nor modification of the charge state distribution has been observed, confirming that no physical degradation, attributable to MS experimental conditions, occurred when fresh infliximab samples were analyzed under these CZE-native MS conditions (Fig. 2).

3.2. *Stressed infliximab analysis*

In the second part of this work, the CZE-native MS method was employed to investigate Infliximab conformational changes induced by a storage stress (6 months at 4 ^{0}C).

The TIC recorded during the analysis of the stressed Infliximab could be divided into three regions (1–3) (Fig. 3A red line). The folded monomer with *m/z* ranging from 5500 to 6700 was detected in the mass spectrum of the three regions of the TIC (Fig. 3B–D). The extracted ion chromatogram (EIC) obtained for the unfolded mAbs signal (3000–5400 m/z) (Fig. 3A, black line) exhibited two peaks, at 4.7 and 5.4 min. On the EIC of the native monomer signal (5500–7500 m/z), a large and tailing peak was observed between 4.5 and 5.4 min (Fig. 3A, blue line). The deconvoluted masses detected in the region 1 are about 150 kDa and 303 kDa, corresponding to the monomer and dimer of Infliximab. The mass spectrum of the region 1 (4.5 min–4.9 min) (Fig. 3B) displayed three envelopes representing, unfolded monomers with *m/z* ranging from 3800 to 5400 and charge state centered at 33+,

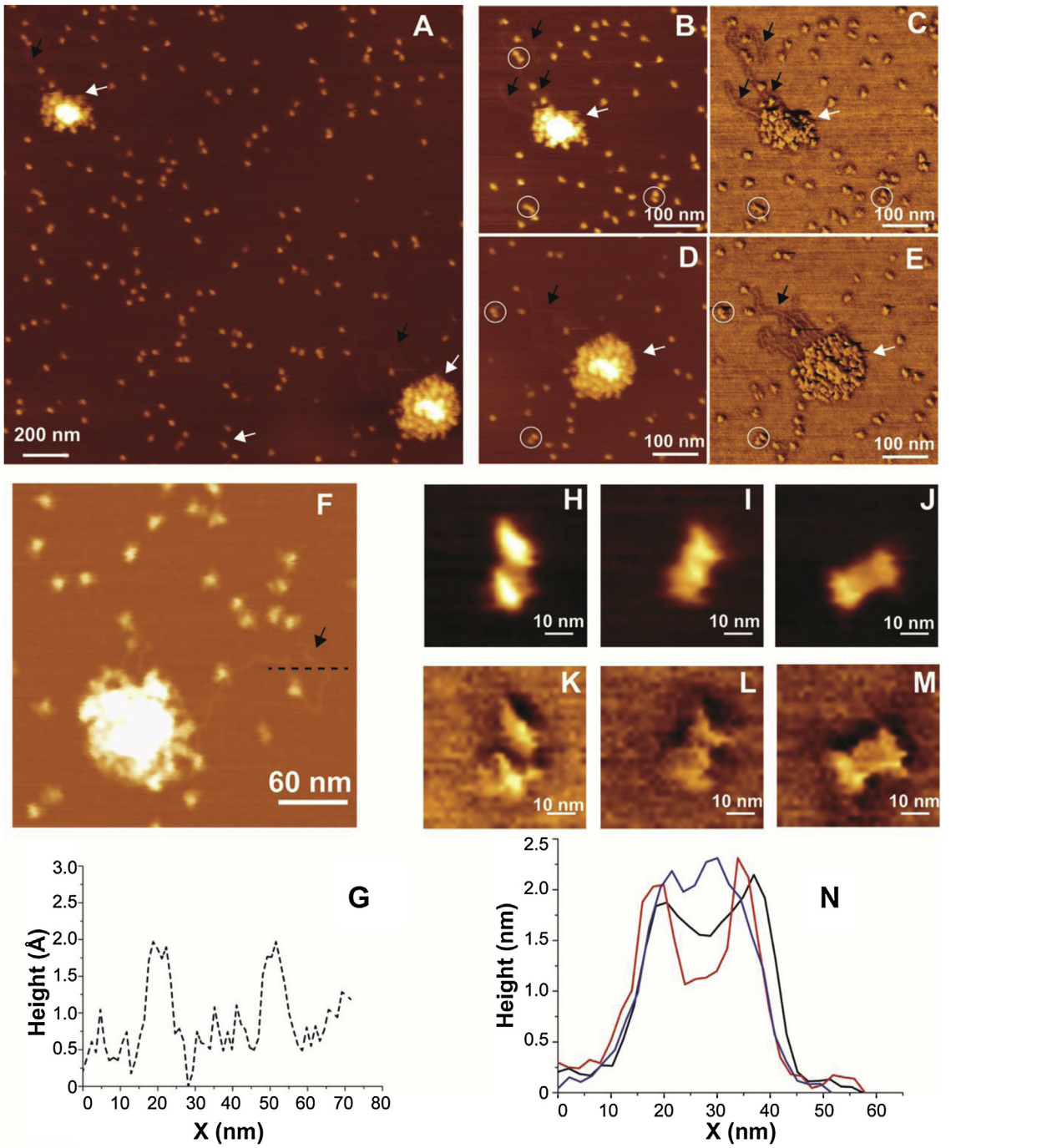


Fig. 6. (A) AM-AFM topography image of stressed Infliximab sample adsorbed onto mica surface performed in ambient conditions. White arrows indicate the presence of aggregates, black arrows point on the protrusions (B), (D), (C) and (E) are topography and phase images of aggregated antibodies with denatured ones. White circles indicate the presence of dimeric forms with different orientation. (F) AM-AFM topography image of an aggregates with a filamentous protrusion (black arrow). Dotted black lines correspond to the line profile plotted in (G). (H)–(J) and (K–M) are topography and phase images of individual dimers forms. (N) line profile of the dimers forms shown in (H)–(J).

a folded monomer (charge state centered at 24+) and a dimer (8000–9000 m/z and charge states centered at 34+). In the mass spectrum of the region 3 (5.3–5.5 min) (Fig. 3D), two possible forms (*m/z* ranging from 3000 to 5400) could be distinguished based on their charge state distributions centered at 33+ ion and 39+, respectively. Considering their similar charge state distribution, we can hypothesize that the unfolded form exhibiting lower charge states (33+) corresponds to the unfolded form detected also in region 1. However, a dimer was detected in region 1 but not in the third one, it exhibits a lower electrophoretic mobility than the monomer. This could be explained by the fact that dimers observed on the region 1 result from a self-association of unfolded forms appearing during the storage (6 months, 4 °C). Then, this dimer could be partially dissociated under our ionization conditions, releasing a small proportion of unfolded monomer during the gas phase process. This suggests that the unfolded mAbs (monomeric form) exhibiting a

charge state centered at 33+ detected in both regions 1 and 3 are related to dimer dissociation and/or non-associated monomers. In region 3, the mass spectrum exhibited an additional unfolded form with charge states centered at 37+. Overall results suggest that CE dimension allows separation of dimers from unfolded monomers and discrimination between two unfolded forms. It is important to note that several partially or fully unfolded mAbs are detected by CE-MS but only the monomer exhibiting a 33+ charge state is prone to self-association during the mAbs storage. This is in agreement with previous works showing that not all the misfolded mAbs are prone to form dimers as this phenomenon is related to amino acid sequences exposed in misfolded mAbs [35].

To characterize the nature of the dimer detected in the stressed mAbs preparation a middle-up approach which included cleavage of the mAb by IdeS below the hinge region to produce $F(ab)_2$ and Fc/2 fragments, and the analysis by the optimized CZE-native MS method, was carried out. After enzymatic digestion of fresh infliximab, CZE analysis showed a poor resolution between (Fab)2 and Fc (Fig. S3). However, CZE dimension was mandatory considering its "online desalting" role before ESI-MS analysis allowing elimination of the digestion buffer (100 mM phosphate pH 7.0). The ESI-MS showed a mass spectrum corresponding to an intact folded $(Fab)_2$ ($\tilde{1}$00 kDa), Fc ($\tilde{5}$1 kDa) fragments which exhibited low charge state distributions centered at 20+, 14+, respectively (Fig. 4A). Very low signals corresponding to small amount of folded undigested Infliximab and Fc/2 ($\tilde{2}$5 kDa) were also observed. The mild conditions of analysis provided by CZE-native MS maintained the non-covalent interactions between the Fc/2 fragment despite the cleavage below the inter-chain disulfide bond [36–38]. A similar observation was made by Haselberg and colleagues [20] when analyzing Infliximab digested by Ides with CE-MS at high acetic acid percentages in BGE (20%). This was attributed by the authors to non-covalent association between the two Fc/2 at acetic acid concentrations below 10%. For the stressed sample, we detected folded signals related to $F(ab)_2$, Fc, Fc/2 and unfolded signals related to $(Fab)_2$ and Fc/2 (Fig. 4B). The unfolded $F(ab)_2$ exhibited the charge state distribution centered at 33+ overlapping the folded Fc and folded Fc/2 signals respectively and exhibited the highest relative abundance percentage (Supplementary data 4). The mass spectrum showed a low relative abundance of unfolded Fc/2. Therefore, we can assume that the dimers observed in stressed mAbs, mostly originate from partially or fully unfolded mAbs present in the initial solution via their unfolded Fab region. These results are in agreement with previous studies describing motifs prone to self-association, in commercial mAbs such as Bevacizumab, Rituximab or Palivizumab [39]. Indeed, several groups have reported mAbs dimers formation via Fab-Fab association in various stressed samples. In most cases, whatever the stress applied UV light exposure [40,41] and temperature [42], Fab-Fab interactions are often demonstrated.

3.3. AFM experiments

In order to confirm that the dimers formation observed by CZE-MS on stressed samples are not artificially formed by the analytical method employed (i.e. ESI conditions), AFM imaging has been performed on Infliximab sample stored 6 months at 4 °C and on fresh infliximab sample. AFM is one of the most powerful tools for the imaging of proteins and their aggregates either in ambient air or physiological conditions with sub-angstrom resolution in vertical direction against a lateral resolution of about 10 nm [25–27,43]. AFM has been widely used in assessing the orientation of immobilized antibodies [44] and their structural changes when exposed to different stressful conditions (salt concentrations, temperature, and adsorption onto hydrophobic substrates) [45,46]. hIn our study we have performed AFM imaging on both Infliximab samples (stored 6 months at 4 °C and fresh) in order to examine the different possible structural morphologies present in the stressed sample and to confirm observation made by CZE-MS on stressed samples.

In fresh Infliximab sample AFM images showed exclusively monomers (Fig. 5A). We can observe from Fig. 5A–E that Infliximab antibodies appear as monomeric features having trinodular structure with a Y-shaped morphology depending on their orientation onto the mica surface. These nodes account to the three IgG fragments (1Fc and 2 Fab). Indeed, whereas the Y-shaped orientation corresponds to the three nodes laying flat on the surface as described in many AFM studies [25–27,43], other antibodies appear with a binodular or monodular shape which corresponds to antibody molecules lying on one side (i.e. either on their Fc or on their two Fab fragments respectively). The isolated antibody structures exhibited a height of 1.5 ± 0.3 nm (n = 220) and a width of 15.8 ± 1.3 nm (n = 80) which are consistent with the values reported in other AFM studies [25–27,43] for IgG monomers (Fig. 5F,G).

In contrast, for the stressed samples, mAbs images revealed in addition to the monomeric form, also dimeric (white circle in Figs. 6A–E), oligomeric (white arrows in Fig. 6B), large aggregates having thin protrusions (black arrows in Fig. 6A–F). All these forms are consequently assumed to be originally present in the stressed sample. The monomeric Infliximab in both samples, stressed and fresh, exhibited similar conformational features. The dimeric structures showed in the topography and phase images (Fig. 6H–N), exhibited a width of 28.7 ± 1.5 nm (n = 13) which corresponds to two monomeric antibodies lying flat and connected to each other. The antibody aggregates revealed a height of 6.7 ± 1.6 nm (n = 22). Such aggregates height corresponded approximately to 4 layers of monomeric antibodies stacked on each other. In addition, the aggregates were frequently surrounded by long filamentous protrusions (Fig. 6G) with a height distribution of 3.2 ± 0.8 Å (n = 14). This low height could correspond to an antibody fully or partially unfolded.

These experiments, performed by AFM, which showed folded monomers, denatured forms and dimers in the stressed sample and only monomers in the fresh sample, are in agreement with those obtained from CZE-native MS. However, it is important to note that the aggregates observed in AFM experiments were not detected by CZE-native MS. This could be due to the high molecular weight of the mAbs aggregates rendering their ionization difficult.

4. Conclusion

We reported in this study a very promising method dedicated to therapeutic mAbs analysis by CZE-native MS. The triple layer coated (PB-DS-PB) capillary is reported for therapeutic mAbs analysis by CZE-native MS for the first time, preventing mAbs adsorption as well as application of additional pressure. In addition, CE could play the role of an on-line desalting method before native-MS. The main advantage compared to SEC is that CZE allows partial separation of different conformational states of Infliximab, and the MS under specific and mild conditions enables the identification of native, unfolded monomers as well as dimers, matching thereby the criteria of a quality control attribute determination. As a proof of concept, the versatility of our approach has been confirmed by analyzing two others therapeutic mAbs. With this new tool, we can anticipate that different stresses provoking mAbs denaturation and dimer formation during their shell life could be further investigated.

The CZE-native MS results concerning mAbs denaturation (partial or total) and dimer formation were confirmed by AFM which evidenced monomers, dimers and unfolded forms in the stressed sample. Importantly, we have demonstrated that the dimer formation observed in our experimental MS conditions was not attributable to the analytical method employed but rather to the

middle term storage of the mAbs. We also demonstrated that the dimer originated from unfolded mAbs via interactions between Fab regions.

Conflict of interest

The authors declare no competing financial interest.

Acknowledgments

We thank the Ecole doctorale "Molécules, Matériaux, Instrumentation et Biosystèmes" which provided the financial support of Victor Le-Minh as a fellowship.

This work was supported in part by ITAAM project (Grant ANR-10-LABX-33, Laboratory of Excellence LERMIT)

The authors would like to thank to Pr. Jean Claude Tabet from CEA Saclay for the valuable discussions about mass spectrometry.

Appendix A. Supplementary data

Supplementary material related to this article can be found, in the online version, at doi:https://doi.org/10.1016/j.chroma.2019.05.050.

References

[1] D.M. Ecker, S.D. Jones, H.L. Levine, The therapeutic monoclonal antibody market, MAbs 7 (2015) 9–14, http://dx.doi.org/10.4161/19420862.2015.989042.
[2] A.M. Scott, J.P. Allison, J.D. Wolchok, Monoclonal antibodies in cancer therapy, Cancer Immun. 12 (2012) (Accessed December 2, 2017) https://www.ncbi.nlm.nih.gov/pmc/articles/PMC3380347/.
[3] K.D. Ratanji, J.P. Derrick, R.J. Dearman, I. Kimber, Immunogenicity of therapeutic proteins: influence of aggregation, J. Immunotoxicol. 11 (2014) 99–109, http://dx.doi.org/10.3109/1547691X.2013.821564.
[4] E.M. Moussa, J.P. Panchal, B.S. Moorthy, J.S. Blum, M.K. Joubert, L.O. Narhi, E.M. Topp, Immunogenicity of therapeutic protein aggregates, J. Pharm. Sci. 105 (2016) 417–430, http://dx.doi.org/10.1016/j.xphs.2015.11.002.
[5] A. Beck, E. Wagner-Rousset, D. Ayoub, A. Van Dorsselaer, S. Sanglier-Cianférani, Characterization of therapeutic antibodies and related products, Anal. Chem. 85 (2013) 715–736, http://dx.doi.org/10.1021/ac3032355.
[6] R. Gahoual, A. Beck, E. Leize-Wagner, Y.-N. François, Cutting-edge capillary electrophoresis characterization of monoclonal antibodies and related products, J. Chromatogr. B 1032 (2016) 61–78, http://dx.doi.org/10.1016/j.jchromb.2016.05.028.
[7] S. Fekete, A.-L. Gassner, S. Rudaz, J. Schappler, D. Guillarme, Analytical strategies for the characterization of therapeutic monoclonal antibodies, TrAC Trends Anal. Chem. 42 (2013) 74–83, http://dx.doi.org/10.1016/j.trac.2012.09.012.
[8] S. Fekete, D. Guillarme, P. Sandra, K. Sandra, Chromatographic, electrophoretic, and mass spectrometric methods for the analytical characterization of protein biopharmaceuticals, Anal. Chem. 88 (2016) 480–507, http://dx.doi.org/10.1021/acs.analchem.5b04561.
[9] R.H. van den Heuvel, A.J. Heck, Native protein mass spectrometry: from intact oligomers to functional machineries, Curr. Opin. Chem. Biol. 8 (2004) 519–526, http://dx.doi.org/10.1016/j.cbpa.2004.08.006.
[10] A.C. Leney, A.J.R. Heck, Native mass spectrometry: what is in the name? J. Am. Soc. Mass Spectrom. 28 (2017) 5–13, http://dx.doi.org/10.1007/s13361-016-1545-3.
[11] M. Tassi, J.D. Vos, S. Chatterjee, F. Sobott, J. Bones, S. Eeltink, Advances in native high-performance liquid chromatography and intact mass spectrometry for the characterization of biopharmaceutical products, J. Sep. Sci. 41 (2018) 125–144, http://dx.doi.org/10.1002/jssc.201700988.
[12] M. Haberger, M. Leiss, A.-K. Heidenreich, O. Pester, G. Hafenmair, M. Hook, L. Bonnington, H. Wegele, M. Haindl, D. Reusch, P. Bulau, Rapid characterization of biotherapeutic proteins by size-exclusion chromatography coupled to native mass spectrometry, MAbs 8 (2015) 331–339, http://dx.doi.org/10.1080/19420862.2015.1122150.
[13] A. Ehkirch, O. Hernandez-Alba, O. Colas, A. Beck, D. Guillarme, S. Cianférani, Hyphenation of size exclusion chromatography to native ion mobility mass spectrometry for the analytical characterization of therapeutic antibodies and related products, J. Chromatogr. B. 1086 (2018) 176–183, http://dx.doi.org/10.1016/j.jchromb.2018.04.010.
[14] T. Ogawa, N. Hirokawa, Multiple analyses of protein dynamics in solution, Biophys. Rev. 10 (2017) 299–306, http://dx.doi.org/10.1007/s12551-017-0354-7.
[15] C. Wenz, C. Barbas, Á. López-Gonzálvez, A. Garcia, F. Benavente, V. Sanz-Nebot, T. Blanc, G. Freckleton, P. Britz-McKibbin, M. Shanmuganathan, F. de l'Escaille, J. Far, R. Haselberg, S. Huang, C. Huhn, M. Pattky, D. Michels, S. Mou, F. Yang, C. Neususs, N. Tromsdorf, E.E.K. Baidoo, J.D. Keasling, S.S. Park, Interlaboratory study to evaluate the robustness of capillary electrophoresis-mass spectrometry for peptide mapping, J. Sep. Sci. 38 (2015) 3262–3270, http://dx.doi.org/10.1002/jssc.201500551.
[16] E.A. Redman, N.G. Batz, J.S. Mellors, J.M. Ramsey, Integrated microfluidic capillary electrophoresis-electrospray ionization devices with online MS detection for the separation and characterization of intact monoclonal antibody variants, Anal. Chem. 87 (2015) 2264–2272, http://dx.doi.org/10.1021/ac503964j.
[17] M. Han, B.M. Rock, J.T. Pearson, D.A. Rock, Intact mass analysis of monoclonal antibodies by capillary electrophoresis—mass spectrometry, J. Chromatogr. B 1011 (2016) 24–32, http://dx.doi.org/10.1016/j.jchromb.2015.12.045.
[18] K. Jooß, J. Hühner, S. Kiessig, B. Moritz, C. Neusüß, Two-dimensional capillary zone electrophoresis-mass spectrometry for the characterization of intact monoclonal antibody charge variants, including deamidation products, Anal. Bioanal. Chem. (2017), http://dx.doi.org/10.1007/s00216-017-0542-0.
[19] A.-L. Marie, G. Rouby, E. Jaccoulet, C. Smadja, N.T. Tran, M. Taverna, Capillary electrophoresis for the quality control of intact therapeutic monoclonal antibodies, Capill. Electrophor. Trends Dev. Pharm. Res. (2017) 305–361, http://dx.doi.org/10.1201/9781315225388-9, Pan Stanford.
[20] R. Haselberg, T. De Vijlder, R. Heukers, M.J. Smit, E.P. Romijn, G.W. Somsen, E. Domínguez-Vega, Heterogeneity assessment of antibody-derived therapeutics at the intact and middle-up level by low-flow sheathless capillary electrophoresis-mass spectrometry, Anal. Chim. Acta 1044 (2018) 181–190, http://dx.doi.org/10.1016/j.aca.2018.08.024.
[21] J. Giorgetti, A. Lechner, E. Del Nero, A. Beck, Y.-N. François, E. Leize-Wagner, Intact monoclonal antibodies separation and analysis by sheathless capillary electrophoresis-mass spectrometry, Eur. J. Mass Spectrom. Chichester Engl. (2018), http://dx.doi.org/10.1177/1469066718807798, 1469066718807798.
[22] A.M. Belov, R. Viner, M.R. Santos, D.M. Horn, M. Bern, B.L. Karger, A.R. Ivanov, Analysis of proteins, protein complexes, and organellar proteomes using sheathless capillary zone electrophoresis - native mass spectrometry, J. Am. Soc. Mass Spectrom. (2017), http://dx.doi.org/10.1007/s13361-017-1781-1.
[23] A.M. Belov, L. Zang, R. Sebastiano, M.R. Santos, D.R. Bush, B.L. Karger, A.R. Ivanov, Complementary middle-down and intact monoclonal antibody proteoform characterization by capillary zone electrophoresis - mass spectrometry, Electrophoresis 39 (2018) 2069–2082, http://dx.doi.org/10.1002/elps.201800067.
[24] R. Haselberg, G.J. de Jong, G.W. Somsen, Capillary electrophoresis of intact basic proteins using noncovalently triple-layer coated capillaries, J. Sep. Sci. 32 (2009) 2408–2415, http://dx.doi.org/10.1002/jssc.200900164.
[25] A. San Paulo, R. García, High-resolution imaging of antibodies by tapping-mode atomic force microscopy: attractive and repulsive tip-sample interaction regimes, Biophys. J. 78 (2000) 1599–1605.
[26] N.H. Thomson, The substructure of immunoglobulin G resolved to 25kDa using amplitude modulation AFM in air, Ultramicroscopy 105 (2005) 103–110, http://dx.doi.org/10.1016/j.ultramic.2005.06.024.
[27] A. Makky, T. Berthelot, C. Feraudet-Tarisse, H. Volland, P. Viel, J. Polesel-Maris, Substructures high resolution imaging of individual IgG and IgM antibodies with piezoelectric tuning fork atomic force microscopy, Sens. Actuators B Chem. 162 (2012) 269–277, http://dx.doi.org/10.1016/j.snb.2011.12.077.
[28] A. Makky, L. Bousset, J. Polesel-Maris, R. Melki, Nanomechanical properties of distinct fibrillar polymorphs of the protein α-synuclein, Sci. Rep. 6 (2016), http://dx.doi.org/10.1038/srep37970.
[29] L. Konermann, D.J. Douglas, Acid-induced unfolding of cytochrome c at different methanol concentrations: electrospray ionization mass spectrometry specifically monitors changes in the tertiary structure, Biochemistry 36 (1997) 12296–12302, http://dx.doi.org/10.1021/bi971266u.
[30] J. Fernandez de la Mora, Electrospray ionization of large multiply charged species proceeds via Dole's charged residue mechanism, Anal. Chim. Acta 406 (2000) 93–104, http://dx.doi.org/10.1016/S0003-2670(99)00601-7.
[31] F. Sousa, B. Sarmento, M.T. Neves-Petersen, Biophysical study of bevacizumab structure and bioactivity under thermal and pH-stresses, Eur. J. Pharm. Sci. Off. J. Eur. Fed. Pharm. Sci. 105 (2017) 127–136, http://dx.doi.org/10.1016/j.ejps.2017.05.019.
[32] J.B. Hedges, S. Vahidi, X. Yue, L. Konermann, Effects of ammonium bicarbonate on the electrospray mass spectra of proteins: evidence for bubble-induced unfolding, Anal. Chem. 85 (2013) 6469–6476, http://dx.doi.org/10.1021/ac401020s.
[33] A.-L. Marie, E. Dominguez-Vega, F. Saller, J.-L. Plantier, R. Urbain, D. Borgel, N.T. Tran, G.W. Somsen, M. Taverna, Characterization of conformers and dimers of antithrombin by capillary electrophoresis-quadrupole-time-of-flight mass spectrometry, Anal. Chim. Acta 947 (2016) 58–65, http://dx.doi.org/10.1016/j.aca.2016.10.016.
[34] F. Foret, T.J. Thompson, P. Vouros, B.L. Karger, P. Gebauer, P. Bocek, Liquid Sheath Effects on the Separation of Proteins in Capillary Electrophoresis/Electrospray Mass Spectrometry, 1994, http://dx.doi.org/10.1021/ac00096a010.
[35] C.J. Roberts, Therapeutic protein aggregation: mechanisms, design, and control, Trends Biotechnol. 32 (2014) 372–380, http://dx.doi.org/10.1016/j.tibtech.2014.05.005.
[36] K. Gunasekaran, M. Pentony, M. Shen, L. Garrett, C. Forte, A. Woodward, S.B. Ng, T. Born, M. Retter, K. Manchulenko, H. Sweet, I.N. Foltz, M. Wittekind, W.

Yan, Enhancing antibody fc heterodimer formation through electrostatic steering effects, J. Biol. Chem. 285 (2010) 19637–19646, http://dx.doi.org/10.1074/jbc.M110.117382.
[37] R.J. Rose, A.F. Labrijn, E.T.J. van den Bremer, S. Loverix, I. Lasters, P.H.C. van Berkel, J.G.J. van de Winkel, J. Schuurman, P.W.H.I. Parren, A.J.R. Heck, Quantitative analysis of the interaction strength and dynamics of human IgG4 half molecules by native mass spectrometry, Structure. 19 (2011) 1274–1282, http://dx.doi.org/10.1016/j.str.2011.06.016.
[38] Y. Leblanc, C. Ramon, N. Bihoreau, G. Chevreux, Charge variants characterization of a monoclonal antibody by ion exchange chromatography coupled on-line to native mass spectrometry: case study after a long-term storage at +5 °C, J. Chromatogr. B 1048 (2017) 130–139, http://dx.doi.org/10.1016/j.jchromb.2017.02.017.
[39] X. Wang, T.K. Das, S.K. Singh, S. Kumar, Potential aggregation prone regions in biotherapeutics, MAbs 1 (2009) 254–267.
[40] R. Paul, A. Graff-Meyer, H. Stahlberg, M.E. Lauer, A.C. Rufer, H. Beck, A. Briguet, V. Schnaible, T. Buckel, S. Boeckle, Structure and function of purified monoclonal antibody dimers induced by different stress conditions, Pharm. Res. 29 (2012) 2047–2059, http://dx.doi.org/10.1007/s11095-012-0732-6.
[41] R. Bommana, Q. Chai, C. Schöneich, W.F. Weiss, R. Majumdar, Understanding the increased aggregation propensity of a light-exposed IgG1 monoclonal antibody using hydrogen exchange mass spectrometry, biophysical characterization, and structural analysis, J. Pharm. Sci. 107 (2018) 1498–1511, http://dx.doi.org/10.1016/j.xphs.2018.01.017.
[42] F. Plath, P. Ringler, A. Graff-Meyer, H. Stahlberg, M.E. Lauer, A.C. Rufer, M.A. Graewert, D. Svergun, G. Gellermann, C. Finkler, J.O. Stracke, A. Koulov, V. Schnaible, Characterization of mAb dimers reveals predominant dimer forms common in therapeutic mAbs, MAbs 8 (2016) 928–940, http://dx.doi.org/10.1080/19420862.2016.1168960.
[43] N.H. Thomson, Imaging the substructure of antibodies with tapping-mode AFM in air: the importance of a water layer on mica, J. Microsc. 217 (2005) 193–199, http://dx.doi.org/10.1111/j.1365-2818.2005.01399.x.
[44] Y.H. Tan, M. Liu, B. Nolting, J.G. Go, J. Gervay-Hague, G. Liu, A nanoengineering approach for investigation and regulation of protein immobilization, ACS Nano 2 (2008) 2374–2384, http://dx.doi.org/10.1021/nn800508f.
[45] H. Lee, M. Kirchmeier, H. Mach, Monoclonal antibody aggregation intermediates visualized by atomic force microscopy, J. Pharm. Sci. 100 (2011) 416–423, http://dx.doi.org/10.1002/jps.22279.
[46] N.A. Barinov, V.V. Prokhorov, E.V. Dubrovin, D.V. Klinov, AFM visualization at a single-molecule level of denaturated states of proteins on graphite, Colloids Surf. B Biointerfaces 146 (2016) 777–784, http://dx.doi.org/10.1016/j.colsurfb.2016.07.014.